

Open Access Article

The authors, the publisher, and the right holders grant the right to use, reproduce, and disseminate the work in digital form to all users.

The Use of Control Angles with MART (Multiplicative Algebraic Reconstruction Technique)

www.tcr.org

MART (Multiplicative Algebraic Reconstruction Technique) is an iterative CT (computed tomography) algorithm [1]. A cycle is completed when all projections have been processed at least once. Iterations of each projection are performed within cycles. In this work, we explore the concept that one or more projections can be iterated multiple times within one cycle. The basic equation is:

$$\rho_{ij}^{q+1} = \rho_{ij}^q \frac{P_{k\theta}}{P_{k\theta}^q} \quad [1]$$

where ρ_{ij}^q is the q^{th} estimate of the grey value ρ for pixel (i,j) , $P_{k\theta}$ is the raysum of the k^{th} ray of the projection at angle θ , which intersects (i,j) , and $P_{k\theta}^q$ is the raysum of the same ray prior to the correction made by Equation [1]. Note that, immediately after application of Equation [1] to a ray, $P_{k\theta}^{q+1} = P_{k\theta}$. In other words, MART forces a match of each ray to its raysum.

MART and other ART algorithms converge at different rates, depending on the order in which the rays are considered. The worst case seems to be considering the angles consecutively, as in our original work (1) and we and others have devised projection orderings that are better than random (2-7), though not yet optimal (8). All projection orderings proposed so far have only used each projection once per cycle. Here we repeat orthogonal pairs of certain projections (cf. (9)) using three ray tracing methods to define the relationship between the pixels and the projection data (10-12), *i.e.*, the weights $w_{ijk\theta}$ in:

$$P_{k\theta} = \sum_{(i,j) \in \text{ray } k} w_{ijk\theta} \rho_{ij} \quad [2]$$

Most of our testing with our C++ test bed software is with fan beams, -120° to 120° , with a projection every 6° , and equal pixel and detector widths. We define a “control pair” to be two mutually perpendicular projections. We considered three “Control Angle” options:

- I. Horizontal/Vertical: The control pair is set to $(0^\circ, 90^\circ)$.
- II. Midpoint: The perpendicular control pair is in the middle of the range of angles. For example in a scan from 0 to 180° , with projections every 6° , the control pair would be $(-45^\circ, 45^\circ)$.
- III. Alternating: Two control pairs are used, the low end pair of right angles, and the high end right angles, in our example $(-120^\circ, -30^\circ)$, and $(30^\circ, 120^\circ)$.

Glen D. Colquhoun¹
Richard Gordon^{1,2,*}

¹Silver Bog Research Inc.
350 Inkster Blvd.
Winnipeg R2W 0K3, Canada
²Dept. of Radiology
University of Manitoba
820 Sherbrook Avenue
Winnipeg R3A1R9, Canada

*Corresponding Author:
Richard Gordon
Email: GordonR@ms.Umanitoba.ca

Key words: MART, Computed tomography algorithms, Projection orderings

Abbreviations: ART, Algebraic Reconstruction Technique; CT, Computed tomography; MART, Multiplicative ART.

For fan beams, when one ray in one projection of a control pair is processed, the corresponding ray in the other projection of the control pair that is close to perpendicular to it is processed next. This improved results compared to sequential processing within each fan beam.

In between the control pairs, we process the remaining projections in one of three different ways:

- I. Sequential processing.
- II. Non-control projection angles are alternated between low and high, working towards the middle.
- III. Non-control projection angles are alternated between low and high, and a third angle oscillating about the center angle is added to the mix. For our example, control angles are processed, then projections 6° , 174° , 84° . Control angles are processed, then projections 12° , 168° , 96° , and so on until each projection is processed.

In each case, the number of non-control projections processed, before returning to the control projections, could be specified. A cycle is complete when all non-control projections have been processed once.

In dealing with reconstruction, we have to be concerned with two sets of values: the range of values of the image, and the range of displayable values. In our case, they both happen to be the same, but this is not always the case. To display values > 255 , we can clip them, *i.e.*, set any value over 255 to 255, or we can apply a factor to all values to bring them into displayable range 0 to 255. We can also constrain the image values when reconstructing, either just the control angles, or the other projection values, or both.

Reconstructions of the Shepp-Logan phantom with the three alternate ray tracing methods, with MART and the three control angle scenarios, for parallel and fan beams, with various numbers of non-control projections processed between control projections, will be shown and compared. The Siddon method works poorly. The use of control angles speeds up convergence.

Acknowledgements

Supported in part by grants from Manitoba Institute for Child Health, Friends You Can Count On, and CancerCare Manitoba.

References

1. Gordon, R., Bender, R., and Herman, G. T. Algebraic Reconstruction Techniques (ART) for Three-dimensional Electron Microscopy and X-ray Photography. *J. Theor. Biol.* 29, 471-481 (1970).
2. Guan, H. and Gordon, R. A Projection Access Order for Speedy Convergence of ART (Algebraic Reconstruction Technique): A Multilevel Scheme for Computed Tomography. *Phys. Med. Biol.* 39, 2005-2022 (1994).
3. Guan, H. and Gordon, R. Computed Tomography Using Algebraic Reconstruction Techniques (ARTs) with Different Projection Access Schemes: A Comparison Study Under Practical Situations. *Phys Med Biol* 41, 1727-1743 (1996).
4. Mueller, K., Yagel, R., and Cornhill, J. F. The Weighted-distance Scheme: A Globally Optimizing Projection Ordering Method for ART. *IEEE Trans Med Imaging* 16, 223-230 (1997).
5. Guan, H., Gordon, R., and Zhu, Y. Combining Various Projection Access Schemes with the Algebraic Reconstruction Technique for Low-contrast Detection in Computed Tomography. *Phys Med Biol* 43, 2413-2421 (1998).
6. Guan, H. and Zhu, Y. Feasibility of Megavoltage Portal CT Using an Electronic Portal Imaging Device (EPID) and a Multi-level Scheme Algebraic Reconstruction Technique (MLS-ART). *Phys Med Biol* 43, 2925-2937 (1998).
7. Guan, H., Gaber, M. W., DiBianca, F. A., and Zhu, Y. CT Reconstruction by Using the MLS-ART Technique and the KCD Imaging System-I: Low-energy X-ray Studies. *IEEE Trans Med Imaging* 18, 355-358 (1999).
8. Gordon, R., Badea, C. T., Colquhoun, G. D., Uytven, E. V., Pistorius, S., Guan, H., and Sargent, E. H. A Contrary View of CTM (Computed Tomographic Mammography): Towards Algorithms and Scanners for 4D Digital Subtraction Screening Mammography. *Technology in Cancer Research and Treatment*, submitted (2004).
9. Kuhl, D. E., Edwards, R. Q., Ricci, A. R., and Reivich, M. Quantitative Section Scanning Using Orthogonal Tangent Correction. *J. Nucl. Med.* 14, 196-200 (1973).
10. Mazur, E. J. and Gordon, R. Interpolative Algebraic Reconstruction Techniques Without Beam Partitioning for Computed Tomography. *Med. Biol. Eng. Comput.* 33, 82-86 (1995).
11. Siddon, R. L. Fast Calculation of the Exact Radiological Path for a Three-dimensional CT Array. *Med Phys* 12, 252-255 (1985b).
12. Gordon, R. A Tutorial on ART (Algebraic Reconstruction Techniques). *IEEE Trans. Nucl. Sci.* NS-21, 78-93, 95 (1974).

BCD Using Ground Penetrating Radar Techniques

www.tcrt.org

In Canada today, one woman in nine can expect to develop breast cancer during her lifetime and one in 25 will die from the disease (Health Canada data). Currently, X-ray mammography is the most effective technique for early stage breast cancer detection. However, due to structure noise and the low contrast between cancer and normal tissue observed in X-ray imagery, mammography yields to a high false negative rate (4%-34%) and a high false positive rate (70%). As a result of these constraints, several alternative approaches for breast imaging have been proposed. Some of them, like MRI or ultrasound, have been shown to be effective for breast cancer detection. However, MRI is too expensive and ultrasound does not have sufficient spatial resolution to be considered for mass screening. In recent years, researchers from the University of Calgary, Dartmouth College, University of Wisconsin-Madison – to name a few – have been investigating the use of microwave imaging technology for Breast Cancer Detection (BCD) purposes. As shown by Surowiec *et al.*, the dielectric properties of cancer and normal tissue exhibit excellent contrast at the microwave frequency range. However, this technique lacks the high spatial resolution provided by X-ray mammography due to its small frequency operation range. As shown by Hagness *et al.*, radar techniques such as confocal imaging, reference subtraction, and surface removal can be successfully used to form Breast Microwave Images (BMI) with a high contrast between cancer and normal tissue.

The motivation of this work is to present an alternative focusing method for breast imaging, coupled with the use of digital signal processing techniques for increasing the spatial resolution in microwave breast imagery. The department of Electrical and Computer Engineering at the University of Manitoba has developed a Stepped Frequency Continuous Wave Ground Penetrating Radar (GPR) test system with a bandwidth of 11 GHz based on a vector network analyzer and a horn antenna that are connected to a PC laptop that uses a GPIB communications protocol. This type of system allows the synthetization of different pulse shapes that can be more appropriate for the application mentioned above. Another advantage of such a type of system is the possibility of working at different operational frequencies that can be more suitable for the different target compositions.

We have investigated the use of the Frequency-wavenumber (F-K) migration technique – a popular method for focusing targets in GPR used by the Geological Sciences community – using a phantom that consists of saline water and a corn syrup mixture to model cancer and breast tissue respectively as suggested by P. M. Meaney of Dartmouth College. This algorithm analyzes the frequency behavior of the scans both in the range and the scan direction in order to converge the scatter responses to its original position on the image. In GPR, the hyperbolic signatures usually seen in GPR images can be collapsed to represent the spatial geometry of for example, a landmine. Essentially, F-K migration is designed to back propagate the wave equation so that the position of a point source or an ensemble of point sources, *i.e.*, the target, can be visualized. The algorithm involves a simple mapping from the frequency domain to the vertical wavenumber by means of an interpolation procedure for the data samples known

Daniel Flores-Tapia¹
Gabriel Thomas^{1,*}
Sima Noghianian¹
Manivannan Poyvasi¹
S. Pistorius²

¹Dept. of Electrical and Computer Engineering

University of Manitoba

Winnipeg, Canada, R3T 6A8

²CancerCare Manitoba

Depts. of Physics and Astronomy & Radiology

University of Manitoba

Winnipeg, Canada R3T 6A8

* Corresponding Author:
Gabriel Thomas
Email: thomas@ee.umanitoba.ca

Key words: Breast cancer detection, Microwave, Ground penetrating radar.

Abbreviations: BCD, Breast Cancer Detection; GPR, Ground Penetrating Radar; BMI, Breast Microwave Images.

as the Stolt interpolation. The F-K algorithm only requires the propagation speed on the medium, and unlike GPR, in BMI this value can be known *a priori*.

In order to increase the spatial resolution of our system, a digital signal processing algorithm based on Auto-Regressive (AR) modeling was used. The coefficients of the AR model were calculated using the Burg method, and the order was obtained using the minimum square error, variance and mean differences between the model output and the original signal. Our initial results have generated focused images with higher resolution when scanning in a configuration similar to stripmap Synthetic Aperture Radar.

With the development of innovative signal and image processing techniques, the ultra wideband microwave system already available in our department has the potential to detect very small cancer tumors before metastasis occurs.

Acknowledgments

The authors would like to thank Stephanie Moorhouse, Department of Microbiology, and Maryam Heshmatzadeh, Department of Electrical and Computer Engineering, both at the University of Manitoba, for their time and help.

A Pseudo-tangential IMRT Technique for the Whole Large Left Breast Radiation Therapy Using Helios/Eclipse System

Huaiqun (Harrison) Guan

Department of Radiation Oncology
Henry Ford Hospital
Detroit, MI 48202

www.tcrt.org

Purpose: To improve the dose uniformity of standard tangential IMRT plan for the whole large left breast radiation therapy.

Materials and Methods: Using the Helios/Eclipse treatment planning system, 6 patients with left breast cancer were planned to receive radiation therapy as a part of their breast conservation therapy following lumpectomy. The separations of these breasts were between 22-26 cm. This is a volume-based inverse planning approach. CT simulation was performed for each patient, and images of 3-mm slices were obtained. The PTV includes the whole breast with 2 cm-sup/inf margins, the posterior margin was along the lung/chest wall border and the medial/lateral wires, and anterior was 3 mm below the skin surface. The PTV contour basically follows the parenchyma. The heart and lung were defined as the organs at risk (OAR). The dose prescribed to the whole breast was 50.4 Gy delivered with 1.8 Gy per fraction. The pseudo tangential IMRT technique (PT-IMRT) basically combines the 4 tangential beams of dual energies (6+18X) with two additional beams angled less than 15 degree from each side. The two additional beams are primarily used to reduce the high dose volume. If the maximum dose is larger than 110%, an additional OAR was drawn at the lateral side. After the inverse optimization, 2 cm skin flash was added to each beam. Multiple static segments were used for the IMRT delivery. The comparisons were made for (i) V95 (volume receiving $\geq 95\%$ relative dose) and V90 for PTV; (ii) V10, V20, V30 and V60 (cc) for heart; (iii) V10, V20, V30, and V40 (cc) for left lung; (iv) the maximum dose; (v) the V105 (cc) (volume receiving doses $\geq 105\%$ in cc) for external; (vii) a reference point dose for the right breast (5 cm right and 1 cm posterior to the P point). The calculation was made for each patient. Besides the PT-IMRT plan, a 3D plan and a tangential IMRT (T-IMRT) plan, both using 4 beams of dual energies, were also generated.

Results: For each patient, the parameters stated above were calculated. The V95 and V90 (especially V95) for PTV were better using the PT-IMRT technique

* Corresponding Author:
Harrison Guan
Email: hquan1@hfhs.org

Key words: Breast cancer treatment, IMRT.

Abbreviations: OAR, Organs at Risk; IMRT, Intensity Modulated Radiation Therapy; CT, Computer Tomography; PTV, Planning Target Volume.

compared to the other two. Most importantly, the V105 (cc) for external was substantially reduced with the technique. The maximum dose of T-IMRT is the largest. The maximum dose of the 3D plan was comparable to PT-IMRT, but its V105 (cc) was usually the largest. Also, for each patient, the V30 for heart and lung was comparable for all three techniques but the V10 and V20 was higher for PT-IMRT compared to T-IMRT and 3D. The V60 (cc) for heart and V40 (cc) for left lung were comparable for all three techniques. The point reference dose to the right breast was about 1.8% higher for the PT-IMRT technique compared to 3D.

Conclusion: The PT-IMRT technique resulted in the most homogenous dose distribution for PTV, the lowest maximum dose for each of the 6 patients. The higher V10 and V20 for the heart and lung are at fairly low doses (at about 5 Gy and 10 Gy, respectively) and as such would be clinically insignificant because the excessive risks for heart and lung were aroused from V60(cc) and V40(cc), respectively. Improved dose distribution thus achieved with PT-IMRT showed less acute effects and is expected to cause less late side effects as well.

Local Independence in Computed Tomography as a Basis for Parallel Computing

www.tcert.org

Advances in computing have reinvigorated Computed Tomography (CT, also known as image reconstruction from projections) as a promising technique for many 3D radiological applications and computed assisted surgery. In CT, an x-ray projection of an object is first taken. The x-ray source emits radiation, and the detector array collects the radiation that is not absorbed and passes through the object. CT estimates the absorption of radiation at each small portion of the object, based on the total amount of radiation detected through each path. Each portion becomes a pixel or voxel in the image representation. Several projections are taken as the x-ray source and detector array rotate around the object, with projections sampled at varying angles. In practice, the projection angles are usually equally spaced and taken in consecutive order, although this need not be the case. Then, using a computer, the image is reconstructed.

There are basically two major categories of image reconstruction algorithms: Fourier (filtered or convolution backprojection) and iterative methods. Fourier methods are based on the fast Fourier transform (FFT) and are derived from the well-known Fourier Slice Theorem (1). These algorithms are based on a frequential decomposition of the data. In many situations, one is restricted in the number of projections (views), in their angular coverage and the number of rays within a view. An example of this is in using CT for screening impending signs on heart attacks. In this case, the motion of the heart limits the number of views that can be taken for any given position of the heart (2, 3). In CTM (CT Mammography), fewer views mean lower dose and higher acceptability for screening. Under these circumstances, iterative techniques have been shown to produce better reconstructions from either few or incomplete views (4) and to produce better performance with noisy and dynamic data. For this reason, iterative techniques are preferred over Fourier based algorithms.

The Algebraic Reconstruction Technique (ART) is one of a variety of iterative reconstruction algorithms. It was the first iterative algorithm proposed for CT (5). ART compares the computed projections or ray sums of an estimated image with the original projection measurements and uses the error obtained from this comparison to correct the estimated image.

Dan Martin¹
Parimala Thulasiraman¹
Richard Gordon^{1,2,*}

Departments of
¹Computer Science
²Radiology
University of Manitoba
820 Sherbrook Avenue
Winnipeg R3A1R9, Canada

* Corresponding Author:
Richard Gordon
Email: gordonr@ms.umanitoba.ca

Key words: Computed tomography, Parallel computing.

Abbreviations: FFT, Fast Fourier Transform; CTM, Computed tomographic mammography.

In routine clinical CT screening, fast Fourier algorithms are the choice by practitioners and manufacturers because iterative algorithms are generally slow. In recent years, however, iterative techniques have been revisited due to the availability of high performance computing making them practical to implement. Wide angle cone beam CT has necessitated a switch to iterative algorithms, and the 3D nature of the reconstructions demands more computer power than ever before.

We have developed a parallel ART algorithm for CT (6). The algorithm has been implemented on a distributed memory architecture using Message Passing Interface (MPI). In this parallel algorithm the projection data is partitioned and distributed to the processors. However, the results were not very impressive. The algorithm produced poor speed due to high overhead in communication between the processors.

A technique that we are currently investigating is a form of localized computed tomography. It is based on our empirical observation that, when one alters one region of a reconstructed image, and then uses the resulting image as the "initial guess" for an iterative CT algorithm, the surrounding regions hardly change at all upon reconvergence (7). In our new approach to parallel CT computation, we partition the image into regions and apply CT within each of the localized regions, using only those rays that pass through the local region, as in local CT (8). Each individual region is distributed to the processors. Several research issues need to be considered: (i) What is the convergence strategy? (ii) Does the algorithm converge? (iii) Since the borders between regions are shared and each region is executed upon by one processor, how often should the computed values in this border be transmitted between the processors? (iv) Is it better to have the local processors address a common stored image? This might avoid the feature of ordinary local CT, which reconstructs a function of the image, rather than the image itself. (v) What is the termination condition? (vi) Should the data be a straightforward

rectangular partitioning or should we alternate with other partitioning strategies, say based on dual graphs? (vii) What size should the partitions be? (viii) How does the computer architecture and its resources such as the speed of the processors, network bandwidth, memory, etc., affect the algorithm?

The search for an effective way to parallelize CT computations must begin in earnest, with the high demands for patient throughput and real-time CT to be met. We think that taking advantage of properties of CT images, such as the partial local independence we have discovered, may be the key to success.

Reference

1. Natterer, F. *The Mathematics of Computerized Tomography*. New York: Wiley (1986).
2. Rangayyan, R. M., A. P. Dhawan, & R. Gordon. Algorithms for Limited-view Computed Tomography: A Survey. In: *Anon., IEEE Int. Conf. on Computers, Systems and Signal Processing*, p. 1540-1545. Bangalore, India: IEEE Press (1984).
3. Rangayyan, R. M., A. P. Dhawan, & R. Gordon. Algorithms for Limited-view Computed Tomography: An Annotated Bibliography and A Challenge. *Applied Optics* 24, 4000-4012 (1985).
4. Guan, H. & R. Gordon. A Projection Access Order for Speedy Convergence of ART (Algebraic Reconstruction Technique): A Multilevel Scheme for Computed Tomography. *Phys. Med. Biol.* 39, 2005-2022 (1994).
5. Gordon, R., R. Bender, & G. T. Herman. Algebraic Reconstruction Techniques (ART) for Three-dimensional Electron Microscopy and X-ray Photography. *J. Theor. Biol.* 29, 471-481 (1970).
6. Melvin, C., P. Thulasiraman, & R. Gordon. Parallel Algebraic Reconstruction Technique for Computed Tomography. In: *Anon., The 2003 International Conference on Parallel and Distributed Processing Techniques and Applications (PDPTA'03: June 23-26, 2003, Las Vegas, Nevada, USA)*, Computer Science Research, Education, & Applications Press (2003).
7. Gordon, R. Artifacts in Reconstructions Made From a Few Projections. In: *Proceedings of the First International Joint Conference on Pattern Recognition, Oct. 30 to Nov. 1, 1973, Washington, D. C., Northridge, California*, Ed., Fu, K.S. IEEE Computer Society, p. 275-285 (1973).
8. Smith, K. T. & F. Keinert. Mathematical Foundations of Computed Tomography. *Applied Optics* 24, 3950-3957 (1985).

A Robotic System for Remote Palpation and Ultrasound Imaging

Farshid Najafi
Nariman Sepehri*

www.tcrt.org

Department of Mechanical and
Manufacturing Engineering
The University of Manitoba
Winnipeg, MB, Canada, R3T 5V6

We have developed an appropriate robotic system capable of performing palpation/ultrasound imaging by an expert at the remote site. Specifically, this work presents the design, development and evaluation of a novel four-degree-of-freedom hand-controller with a force reflecting capability and a novel four-degree-of-freedom wrist mechanism to assist the physician in performing abdominal and breast examinations such as palpation and ultrasound imaging from a remote site.

* Corresponding Author:
Nariman Sepehri
Email: nariman@cc.umanitoba.ca

Key words: Robotic, Breast, Palpation, Ultrasound.

A compact desktop four degree-of freedom spherical parallel hand-controller has been designed with back-drivability, large and singularity-free workspace, and force reflecting capability. The structure is light, yet rigid, and the actuators are all placed on the base, providing independent control of each degree of freedom. All degrees of freedom are kinematically decoupled from each other. The first two degrees-of-freedom are generated by two identical pantographs pivoted together to provide a hemispherical motion of a handle about an interior fixed point. The third degree-of-freedom represents a sliding motion along the created hemisphere. The fourth degree-of-freedom represents the rotational motion of the handle. The operator is able to control the position and orientation of a remote wrist holding an ultrasound or a palpating probe and receive the interaction forces between the patient and the probe at the remote site. A simplified version of this design with three degrees of freedom has been fabricated (see Fig. 1).

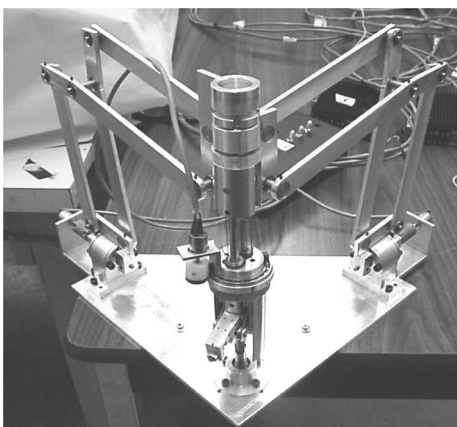


Figure 1: General view of the hand-controller.

A compact, spherical, parallel, modular, robotic wrist with four degrees of freedom has also been designed, having simi-

lar unique characteristics as in the hand-controller. The wrist has two exchangeable modules to provide standard clinical motions for palpation and ultrasound imaging. The first two degrees-of-freedom are generated by two identical pantographs pivoted together to define a hemispherical motion of a probe about an exterior fixed point. The third degree-of-freedom is linear motion along the radius of created hemisphere. The fourth degree-of-freedom is a rotational motion of the probe about the radius of the created hemisphere. A simplified prototype of the design having three degrees of freedom has been constructed (see Fig. 2). Due to the type of its movements, the developed prototype is presently most suitable for performing ultrasound examination.

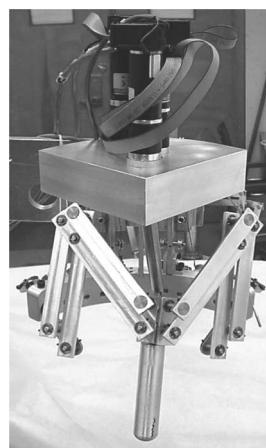


Figure 2: General view of the robotic wrist.

Both systems are interfaced to a computer and simple control schemes have been applied for controlling them. When operated together, both mechanisms are kinematically similar. This property simplifies control algorithms, increases force transparency and generates a user-friendly robotic system for tele-medicine applications.

Ultra-Wide-Band Radar for Early Breast Tumor Detection

www.tcrt.org

M. Poyvasi¹
S. Noghianian^{1,*}
G. Thomas¹
D. Flores¹
S. Pistorius²

Breast cancer is the leading cause of morbidity and mortality among women in many parts of the world, and it is the major cause of cancer death among women, next only to lung cancer (1). Early detection and timely medical intervention are two key factors that impact long-term survival and quality of life of breast cancer patients. X-ray mammography remains the primary screening method for detecting non-palpable early-stage breast tumors. However, despite significant progress on mammographic techniques, well-recognized limitations do persist (2). Magnetic Resonance Imaging (MRI) has shown promise as a Breast Imaging technology, but it has its shortcomings as a screening tool due to its limited availability and its failure to distinguish between cancerous and non-cancerous abnormalities. There are two key scientific requirements needed for any imaging technique to be accepted as a robust screening tool: i) high detection rate, so that correct classification of women with cancer can be obtained, and ii) specificity, which deals with proper determination of the type of the cancer, and how far it has spread. So far, no single imaging modality or method has both high sensitivity and specificity for this disease. With this background, this modality, namely, microwave imaging using very low power microwave signals (comparable to that of our present day cell phones), sensitive to tumors and specific to malignancies shows promise for the early detection and screening of breast tumors.

This work is related to active microwave imaging that exploits the significant dielectric contrast between malignant breast tumor and normal breast tissue. As a forerunner of an ongoing experimental investigation on microwave scattering (3) in a multilayered breast phantom using ultra-wideband (UWB) ground penetrating radar (GPR) system at the Department of Electrical and Computer Engineering, University of Manitoba, this simulation study was performed in both time domain (TD) and frequency domain (FD).

A hemispherical breast model with a spherical tumor was simulated using FEKO, a commercial Method of Moment package for electromagnetics simulation. A Gaussian pulse was used for excitation (E_{iz}) defined by: $E(t) = \exp\{-a(t-t_0)^2\}$, where $a = 13E09(s^{-1})$ and $t_0 = 6$ (ns). The time response died out within 40 light-metre or 133 ns. The permittivity chosen for the early tumor was 16 and that of the normal tissue was 8, to comply with the ratio needed for the contrast. Other pertinent data: $\sigma_{\text{tumor}} = 1.72$ S/m, $\sigma_{\text{normal}} = 0.87$ S/m, Diameter_(Hemisphere) = 90 mm and Diameter_(Tumor) = 5 mm. TD-FD simulations for the backscattered near-field for this near-field imaging modality with time-in-points, were obtained. Specific absorption rate (SAR) obtained for hemispheres with tumor and without a tumor validates the multicompartamental dielectric losses (using surface equivalent principle) in this simulation study while meeting the standard C95.1-1999 for SAR.

Acknowledgments

The authors would like to thank Stephanie Moorhouse, Department of Microbiology, and Maryam Heshmatzadeh, Department of Electrical and

¹Department of Electrical and Computer Engineering
²CancerCare Manitoba
Departments of Physics and Astronomy, & Radiology
University of Manitoba
Winnipeg, Manitoba
R3T 5V6, Canada

* Corresponding Author:
Sima Noghianian
Email: sima@ee.umanitoba.ca

Key words: Breast cancer detection, Microwave, Ultra-wide-band radar.

Abbreviations: BCD, Breast Cancer Detection; UWB, Ultra-wide-band; GPR, Ground Penetrating Radar.

Computer Engineering both at the University of Manitoba, and Ujwala Manivannan for their time and help.

References

1. Liu, L. *Breast Cancer Overview*. Oncolink, Univ. of Penn. Cancer Center (1999).
2. *Mammography and Beyond: Developing Techniques for the Early Detection of Breast Cancer*. Washington, DC: Inst. Med., Nat. Academy Press (2000).
3. Kong J. Au. *Electromagnetic Wave Theory, 2nd Edition*. New York: John Wiley & Sons (1990).

Image Quality Assessment of Fused Full Field Digital Mammography and Ultrasound Imaging System (FFDMUS)

www.tcrt.org

Ultrasound and X-ray images can be acquired simultaneously using a prototype FFDMUS system, which combines both modalities in a single gantry. The value of such a system is predicated on the assumption that there is no loss of image quality as a result of the combination. It is necessary to validate this assumption before the FFDMUS device can be developed for clinical screening or diagnosis. This paper presents the initial results of phantom-based measurements of ultrasound and X-ray image quality in the fused FFDMUS framework.

To assess ultrasound image quality, we measured axial and lateral resolution by means of point spread function (PSF) analysis. In addition, measurements of transmission loss and near field ring-down artifact were made and compared to an equivalent handheld ultrasound transducer (HHUS). Finally, a spherical void phantom with 3 mm and 5 mm diameter cystic lesions was used to measure the area of the observed lesion and compared that with the ideal lesion. For the X-ray image quality assessment, we measured the Modulation Transfer Function (MTF), Detective Quantum Efficiency (DQE), and Normalized Noise Power Spectrum (NNPS) of the FFDMUS and compared that to SenoScan® FFDM.

The FFDMUS prototype demonstrated ultrasound image quality comparable to HHUS in lateral resolution and transmission loss (<5dB). The acoustic coupler used in the FFDMUS system resulted in a minor loss of axial resolution (at the -30dB level) and in an increase (from 1.7mm to 3.8mm) in ring-down artifact. These differences can be corrected by design changes to the acoustic coupler. The spherical lesion analysis in ultrasound images showed that FFDMUS and HHUS were comparable. In X-ray mammograms, the comparison between from the prototype FFDMUS and product-qualified SenoScan® FFDM demonstrated equivalent performance in terms of resolution, fine-detail visibility, noise and contrast.

Jasjit Suri^{1,*}
Yujun Guo²
Tim Danielson¹
Cara Coad¹
Idris Elbakri¹
Rob Entrekkin³
Alex Kwan⁴
John Boone⁴
Roman Janer¹

¹Fischer Imaging Corporation
Denver, CO 80241

²Kent State University
Kent, OH 44242

³Philips Medical Systems
Bothell, WA 98041-3003

⁴University of California
Davis, CA 95616

* Corresponding Author:
Jasjit Suri
Email: JSuri@fischerimaging.com

Key words: Digital mammography, Image quality assessment.

Evaluation of a New FFDM SenoScan Review Workstation Based on Nine-Mega Pixel Flat Panel Display & Windows OS at Fischer Imaging

www.tcrt.org

We demonstrate the feasibility of “Nine-Mega Pixel Flat Panel Display Monitors” (LCDs) for mammography applications in Windows OS framework at Research and Development Division, Fischer Imaging Corporation, Denver, Colorado.

Our NIH research funded grant was used for physics characterization of the flat panel LCD monitor. During the experimentation, we computed MTF, noise and resolution. The MTF was determined using an established method (Samei *et al.*, *Medical Physics* 25, 102-113, 1998). In this method, the angle of each line was determined precisely, and the image data re-projected along the line to form the line-spread function (LSF). The LSF was smoothed by a moving polynomial fit, base-line corrected, filtered by a Hanning filter, Fourier transformed, and normalized to obtain the MTF.

For the NPS evaluation, the camera was focused on the central uniform area of the TG18-RN50 test pattern. The NPS was determined using an established method (Flynn and Samei, *Medical Physics* 26, 1612-1623, 1999). In this method, the image was segmented into 56 128×128 ROIs. Each ROI was converted to relative values, detrended by a two-dimensional polynomial fit, filtered by a Hamming filter, Fourier transformed, and normalized to obtain the ROI NPS. The NPS from different ROIs were then averaged, and orthogonal and radial frequency bands extracted to obtain the 1-D NPS results.

We also ported our SenoScan architecture based on Unix OS to Windows OS first time with user-friendly features. We conclude the following: (a) FP-LCD has higher MTF and resolution and higher structured noise. Notwithstanding the perceptual impact of structured noise, on which there is currently no consensus in the scientific community, the resolution and noise results suggest that the LCD panel is suitable for use in mammography applications, particularly taking into consideration its superior resolution performance. In terms of noise, it is highly likely that the human visual system might be able to pre-whiten the noise structure associated with the pixilated pattern of the LCD lay, reducing the potential impact of the structured noise. (b) The overall system performs smoothly and is currently undergoing more tests and feature additions for dual-displays along with clinical trials.

Key words: FFDM, Evaluation.

Abbreviations: FFDM, Full field digital mammography; MTF, Modulation transfer function; ROI, Region of interest.

Jasjit S. Suri^{1,*}
Tom Minyard¹
Ron Woodward¹
Idris Elbarki¹
Eshan Samei²
Kai Schleupen²
Susan Coley³
Steeve Wright³
Roman Janer¹

¹Fischer Imaging Corporation
Denver, Colorado

²Duke University
Durham, NC 27708

³IBM TJ Watson Research Center
New York 10604

* Corresponding Author:
Jasjit S. Suri
Email: JSuri@fischerimaging.com